Available online at www.sciencedirect.com

ScienceDirect

Procedia IUTAM 10 (2014) 263 – 272

Procedia IUTAM

www.elsevier.com/locate/procedia

23rd International Congress of Theoretical and Applied Mechanics

Dynamics of marine ice sheets

M. Grae Worster*

Institute of Theoretical Geophysics, Department of Applied Mathematics and Theoretical Physics, University of Cambridge, CMS Wilberforce Road, Cambridge CB3 0WA, UK

Abstract

Marine ice sheets, which are those that terminate in the ocean forming a floating ice shelf, dominate the ice sheets of West Antarctica, where much of the bedrock is below sea level. The weight of the thick ice sheets keep them in contact with the bedrock until they are thin enough to float on the ocean as ice shelves. This paper reports mathematical models and associated laboratory studies of analogue systems using either Newtonian or shear-thinning viscous fluids to represent flowing ice. It is shown that the rheology has little influence on the qualitative behaviour of grounded flows but floating, shear-thinning shelves are found experimentally to be subject to a fingering instability reminiscent of features seen in Antarctic ice shelves.

Selection and/or peer-review under responsibility of the Organizing Committee of The 23rd International Congress of Theoretical and Applied Mechanics, ICTAM2012

Keywords: ice sheets, thin-film flows, extensional flows

1. Introduction

In the decade 1993 to 2003, global sea level rose by almost 3 mm yr^{-1}. More than half of this rise can be attributed to thermal expansion of the oceans and most of the rest to melting of glaciers and ice sheets. Predictions made in the most recent IPCC report are for a similar rate of sea-level rise in the next hundred years, leading to a total rise of a few tens of centimetres. Estimates of the rates at which terrestrial ice sheets will melt can be made fairly reliably given predictions of atmospheric warming. However, the flow and possible collapse of marine ice sheets are much harder to predict. There is therefore much current research devoted to understanding the physical controls on the flow of marine ice sheets and to understanding their stability at the grounding line where they detach from bedrock to form floating shelves. This article illustrates some of the fundamental fluid-mechanical controls on the flow of grounded sheets and floating shelves using simple laboratory analogues and associated mathematical modelling.

On large, continental scales, ice flows as a viscous, non-Newtonian fluid. It is most commonly modelled using Glen's flow law, which treats the ice as a simple, shear-thinning fluid in which the viscous stresses are proportional to a power $1/n$ of the rate of strain, with n often taken equal to 3. For much of the discussion here, we shall treat ice as a Newtonian fluid, for which $n = 1$, but we shall consider the effects of $n > 1$ towards the end of the article.

*Corresponding author. *E-mail address:* grae@damtp.cam.ac.uk.

2210-9838 © 2013 Published by Elsevier Ltd. Open access under CC BY-NC-ND license.
Selection and/or peer-review under responsibility of the Organizing Committee of The 23rd International Congress of Theoretical and Applied Mechanics, ICTAM2012
doi:10.1016/j.piutam.2014.01.022

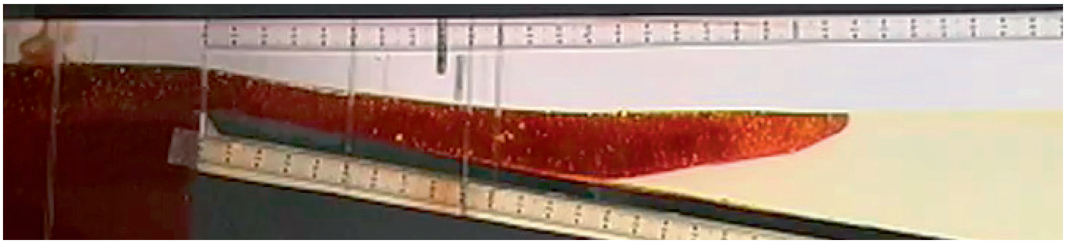

Fig. 1. A laboratory experiment in which golden syrup flows down a sloping bed into a denser layer of potassium carbonate solution.

This account of the presentation given at ICTAM 2012 is based on the papers listed in the bibliography at the end [1–5]. References to the associated literature can be found in those papers.

2. Newtonian modelling of two-dimensional sheets and shelves

A laboratory experiment that illustrates the geometry of a two-dimensional, sheet–shelf system is shown in Fig. 1. Viscous golden syrup is introduced at a constant rate at the top of a rigid slope and forms a flow that is initially grounded on the slope. At some distance from the source, the flowing syrup detaches from the slope to form a floating shelf. The locus of detachment is the grounding line.

The grounded part of the flow forms a type of viscous gravity current, which have been studied extensively and are reviewed here briefly in the context of two-dimensional flow along a horizontal, rigid boundary. In such flows, illustrated in Fig. 2a, the dominant force balance is between horizontal gradients in hydrostatic pressure and viscous stresses associated with vertical shear. This balance is represented within a thin-film approximation by

$$\rho g \frac{\partial h}{\partial x} \approx \mu \frac{\partial^2 u}{\partial y^2}, \tag{1}$$

where $u(x, y, t)$ is the horizontal velocity of the current, $h(x, t)$ is the height of its free surface, ρ and μ are its density and dynamic viscosity, and g is the acceleration due to gravity. Equation (1) can be integrated subject to no slip at the base $y = 0$ and no stress at the upper surface $y = h$ to give the parabolic velocity profile

$$u = -\frac{g h_x}{2\nu} y(2h - y), \tag{2}$$

where $\nu = \mu/\rho$ is the kinematic viscosity and $h_x \equiv \partial h/\partial x$. The associated horizontal volume flux is

$$q \equiv \int_0^h u \, \mathrm{d}y = -\frac{g h^3 h_x}{3\nu}, \tag{3}$$

which can be used within the continuity equation

$$\frac{\partial h}{\partial t} + \frac{\partial q}{\partial x} = 0 \tag{4}$$

to give a nonlinear diffusion equation for the thickness of the flow

$$\frac{\partial h}{\partial t} = \frac{g}{3\nu} \frac{\partial}{\partial x}\left(h^3 \frac{\partial h}{\partial x}\right). \tag{5}$$

This equation can be solved given the source condition $q = q_0$ at $x = 0$ and a second condition that, when the flow evolves self-similarly, is often expressed as an integral constraint on the volume of the current. However, for more general situations it is necessary to provide an evolution equation for the position of the end of the current, which can be determined from consideration of conservation of mass in a small control volume around the end of the current to be

$$\dot{x}_{N,\mathrm{kin}} = \lim_{x\to x_N} \frac{q}{h} = -\frac{g}{3\nu}h^2 h_x. \tag{6}$$

This kinematic evolution equation expresses the fact that the current simply advances at the rate at which material is supplied to the end of it.

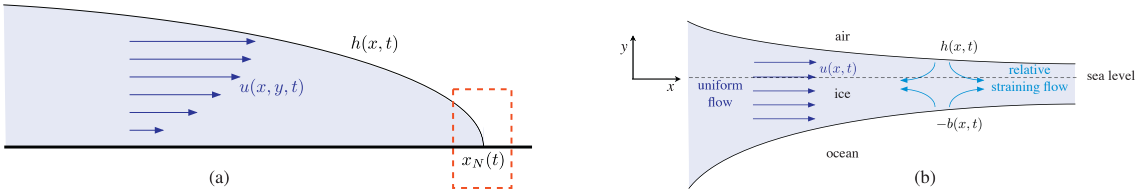

Fig. 2. Schematic diagrams of (a) a viscous gravity current on a rigid surface and (b) a floating, viscous extensional gravity current.

In contrast with the shear-dominated sheet, the leading-order flow in the shelf is vertically uniform but undergoes longitudinal strain, as illustrated in Fig. 2b. Its horizontal velocity $u(x,t)$ satisfies an elliptic equation

$$2\mu\frac{\partial}{\partial x}\left(H\frac{\partial u}{\partial x}\right) = \frac{\rho g'}{2}H\frac{\partial H}{\partial x}, \tag{7}$$

where $g' = (\rho_w - \rho)/\rho_w$ and ρ_w is the density of the ocean, coupled with a hyperbolic equation

$$\frac{\partial H}{\partial t} + \frac{\partial}{\partial x}(Hu) = 0 \tag{8}$$

for its thickness $H(x,t)$. These equations can be solved given a source condition of constant flux $q = q_0$ at $x = x_0$ to show that

$$H = H_0\left[1 + g' H_0^2(x - x_0)/4\nu q_0\right]^{-1/2}, \tag{9}$$

independent of time: the fluid simply fills a constant envelope with the front accelerating according to

$$x_N - x_0 = \frac{q_0}{H_0}t + \frac{g'}{16\nu}q_0 t^2, \tag{10}$$

where $H_0 = H(0,t)$ is prescribed to be constant.

The shelf floats on the ocean and we make the assumption that it is in simple Archimedian balance. In particular, we assume that this balance is achieved in the sheet at the grounding line so that

$$h(x_G(t), t) = \frac{\rho_w}{\rho}\frac{g'}{g}b(x_G(t)), \tag{11}$$

which can be differentiated with respect to time to determine an evolution equation for the grounding line

$$\frac{\partial h}{\partial x}\dot{x}_G + \frac{\partial h}{\partial t} = \frac{\rho_w}{\rho}\frac{g'}{g}\frac{\mathrm{d}b}{\mathrm{d}x}\dot{x}_G, \tag{12}$$

where the spatial derivatives are taken in the sheet. This equation relates changes in position of the grounding line to thickening or thinning of the sheet there.

A longitudinal force balance across the grounding line

$$4\mu\frac{\partial q}{\partial x} + 2\rho g H^2\left(\frac{\partial h}{\partial x}\right)^2 = \tfrac{1}{2}\rho g' H^2 \tag{13}$$

can be applied given a questionable assumption that viscous bending stresses are negligible at the grounding line. Part of the motivation of the experiments described below is to test the validity of such assumptions in models of marine ice sheets coupled dynamically to floating ice shelves through their grounding lines.

The previous two equations can be combined to determine an equation for the dynamic evolution of the grounding line

$$\left(\frac{\rho_w}{\rho}\frac{g'}{g}\frac{\mathrm{d}b}{\mathrm{d}x} - \frac{\partial h}{\partial x}\right)\dot{x}_{G,\mathrm{dyn}} = \frac{gH^2}{2\nu}\left(\frac{\partial h}{\partial x}\right)^2 - \frac{g'H^2}{8\nu}. \tag{14}$$

In certain circumstances, this equation predicts that the grounding line advances more quickly than material can be supplied to it from the sheet. In such circumstances, a shelf cannot form and the edge of the sheet is predicted to advance kinematically according to Eq. (6).

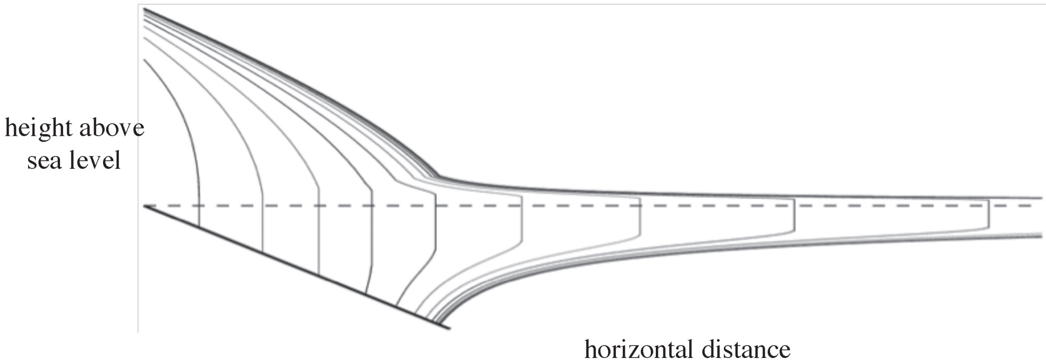

Fig. 3. Computational results for the evolution of a two-dimensional sheet–shelf system on a uniform slope, fed by a constant flux. Note that the shelf advances some way before a shelf forms and that a steady state is reached eventually.

Equations similar to Eqs. (5) – (8) can be solved numerically to determine the profiles shown in Fig. 3 for viscous fluid introduced at constant rate at sea level at the top of a uniform slope of gradient α. It can also be determined that $x_G \propto t^{4/5}$ at early times and tends to a steady value

$$x_G = \frac{1}{\alpha}\frac{\rho}{\rho_w}\left(\frac{6\nu q_0}{g}\right)^{1/3}\left(\frac{g}{g'}\right)^{1/6} \tag{15}$$

as $t \to \infty$. This latter prediction was compared with the maximum run-out distance of grounding lines in experiments similar to that shown in Fig. 1. The parametric dependences in Eq. (15) gave some correlation of the experimental data but generally underpredicted the experiments. The mismatch was suggested to be due to the rise in sea level caused by the addition of the viscous fluid and to horizontal shear stresses in the shelf due to its contact with the rigid side walls of the experimental tank.

3. Newtonian modelling of axisymmetric shelves

It is relatively straightforward to ensure experimentally that the level of the inviscid fluid (sea level) is maintained constant. On the other hand, the horizontal stresses exerted on a shelf confined to a channel or bay are an important aspect of natural ice shelves, giving stability to the grounding line by buttressing the ice sheet. Nevertheless, in an effort to understand the dynamical evolution of grounding lines without the added complications of horizontal shear, we have carried out a systematic study of axisymmetric sheet–shelf systems, as illustrated in Fig. 4.

An axisymmetric shelf is a relatively simple example of a general three-dimensional shelf, whose depth-integrated properties can be determined from the two-dimensional equations

$$\nabla(\mu H \nabla\cdot\boldsymbol{u}) + \nabla\cdot(\mu H \boldsymbol{e}) = \frac{\rho g'}{2}H\nabla H, \tag{16}$$

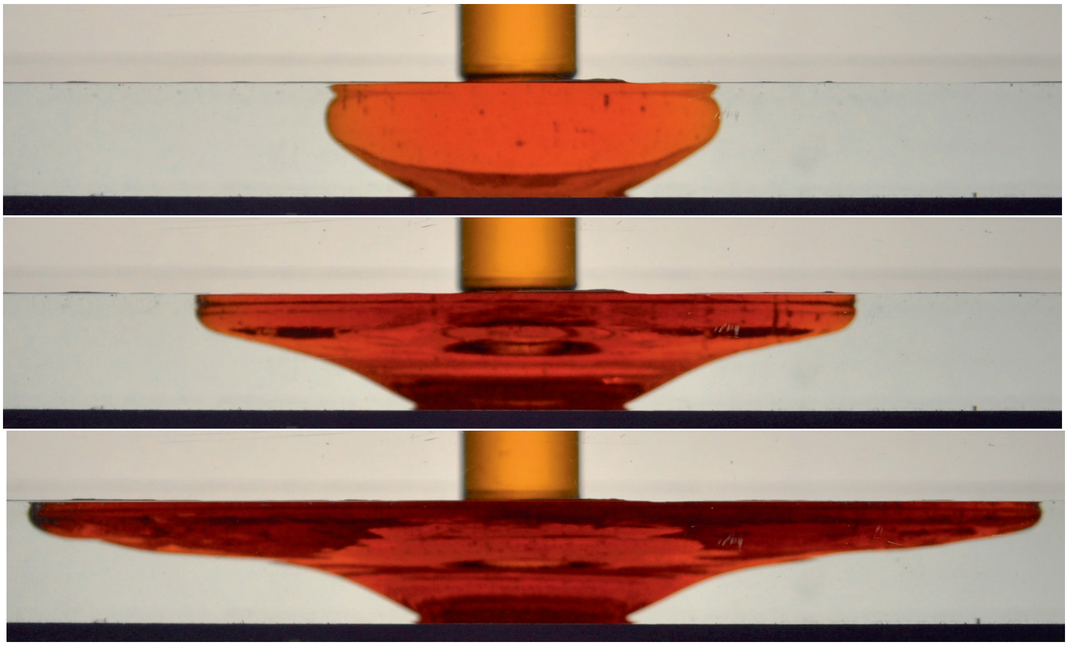

Fig. 4. The evolution of an axisymmetric sheet–shelf system of golden syrup introduced into a denser layer of potassium carbonate solution.

$$\frac{\partial H}{\partial t} + \nabla \cdot (H\boldsymbol{u}) = 0. \tag{17}$$

The axisymmetric forms of these equations

$$\frac{\partial}{\partial r}\left[H\left(2\frac{\partial u}{\partial r} + \frac{u}{r}\right)\right] + H\frac{\partial}{\partial r}\left(\frac{u}{r}\right) = \frac{g'}{2\nu}H\frac{\partial H}{\partial r}, \tag{18}$$

$$\frac{\partial H}{\partial t} + \frac{1}{r}\frac{\partial}{\partial r}(rHu) = 0 \tag{19}$$

can be solved subject to source conditions at a radial origin

$$\lim_{r\to 0}(2\pi rHu) = Q_0, \qquad H(0,t) = H_0, \tag{20}$$

where Q_0 and H_0 are constants, and front conditions

$$2\frac{\partial u}{\partial r} + \frac{u}{r} = \frac{g'}{4\nu}H, \qquad \dot{r}_N = u \qquad (r = r_N). \tag{21}$$

Solutions to these equations, which are illustrated in Fig. 5, reveal interesting dynamical balances. Asymptotic analysis shows that at early times the flow is purely extrusional: buoyancy forces are negligible and the front advances under a balance of radial and azimuthal viscous stresses such that

$$r_N \sim \eta_N \left(\frac{Q_0}{2\pi H_0}t\right)^{1/2}, \qquad t \to 0, \tag{22}$$

where η_N is a constant. As time progresses, the viscous shelf reaches a steady state $H(r,t) \sim H(r)$ near the source, $r \ll r_N$, though the greater proportion of the shelf remains time dependent, governed by a balance between buoyancy and viscous forces and spreading self-similarly with

$$r_N \sim \xi_N \left(\frac{Q_0 g'}{2\pi\nu}\right)^{1/2} t, \qquad t \to \infty, \tag{23}$$

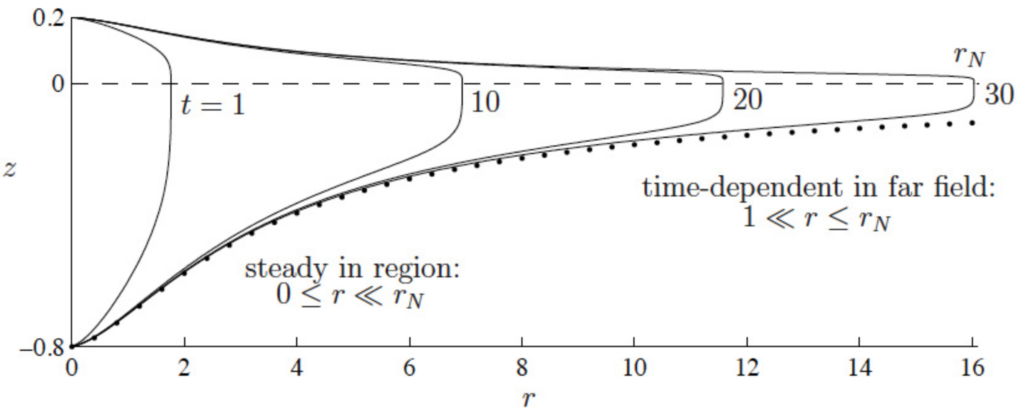

Fig. 5. The computed evolution of an axisymmetric, floating shelf

where ξ_N is a constant. This latter expression gives excellent predictions of controlled laboratory experiments, as shown in Fig. 6. The experiments are challenging because, on the laboratory scale, surface tension exerts a significant force on the shelf. This was overcome by creating viscous shelves along the interface between two relatively inviscid aqueous fluids of different densities.

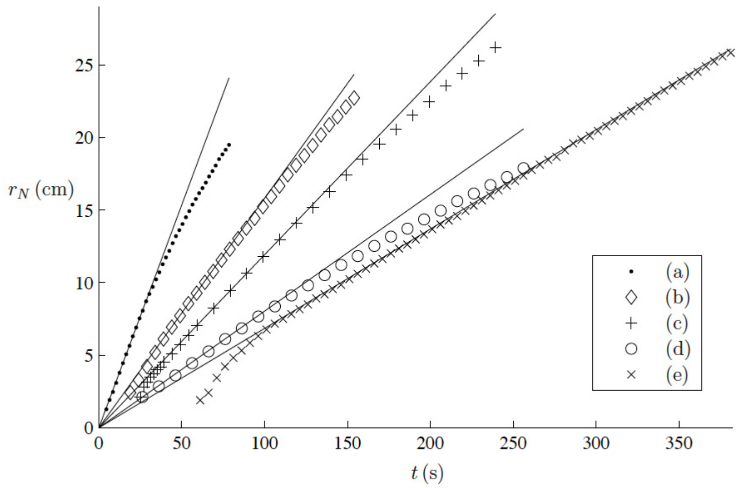

Fig. 6. Comparison between experimental data and theoretical predictions for the extent of a floating shelf fed by a constant flux.

4. Newtonian modelling of axisymmetric, coupled sheets and shelves

The modelling of axisymmetric, grounded sheets follows that of axisymmetric, viscous gravity currents and is structurally similar to the modelling of two-dimensional sheets. It is a special case ($n = 1$) of the modelling of power-law, viscous gravity currents presented below. The equations governing the sheet can be coupled to those describing the shelf, presented in the previous section, by employing the same physical considerations that were described in Sect. 2. These lead to the dynamical equation

$$\left(-\frac{\partial H}{\partial r}\right)\dot{r}_{N,\mathrm{dyn}} = \frac{g}{2\nu}H^2\left(\frac{\partial h}{\partial r}\right)^2 - \frac{g'}{8\nu}H^2 - \frac{q}{2r} - \frac{1}{2}\int_{r_G}^{r_N} H\frac{\partial}{\partial r}\left(\frac{u}{r}\right)\,\mathrm{d}r. \tag{24}$$

The first two terms on the right-hand side represent the same dynamical components that were present in two dimensions. The third term relates to thinning of the sheets associated with radial spreading. The final term includes the viscous hoop stresses in the shelf created as material in the shelf is stretched azimuthally. Note particularly that the grounding line is influenced by the accumulated (integrated) hoop stresses within the whole shelf, not just by local viscous stresses.

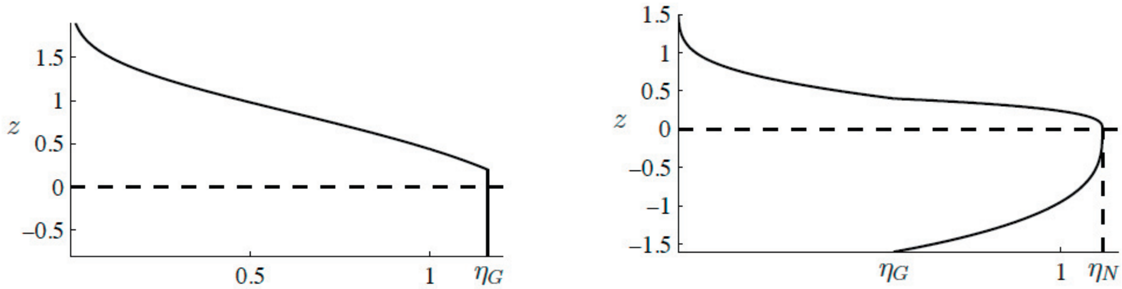

Fig. 7. The early time structure of a gravity current introduced into a layer of denser, inviscid fluid. If the layer is shallow (left) then a sheet forms with no shelf. If the layer is deeper (right) then a shelf can form from the outset.

Buoyancy and viscous forces are involved from the outset, combined in a similarity solution in which

$$r_{G,N} = \eta_{G,N} \left(\frac{\nu Q_0}{2\pi g} \right)^{3/8} \left(\frac{g}{\nu} \right)^{1/2} t^{1/2}, \tag{25}$$

where $\eta_{G,N}$ are constants. Depending on the dimensionless depth of the ocean $D = b_0(\rho_w/\rho)(2\pi g/\nu Q_0)^{1/4}$, the shelf can either form straight away (in a relatively deep ocean) or the sheet advances kinematically until the radial viscous forces within it have reduced sufficiently to balance the hydrostatic force of the (relatively shallow) ocean. These two forms of early-time behaviour are illustrated in Fig. 7.

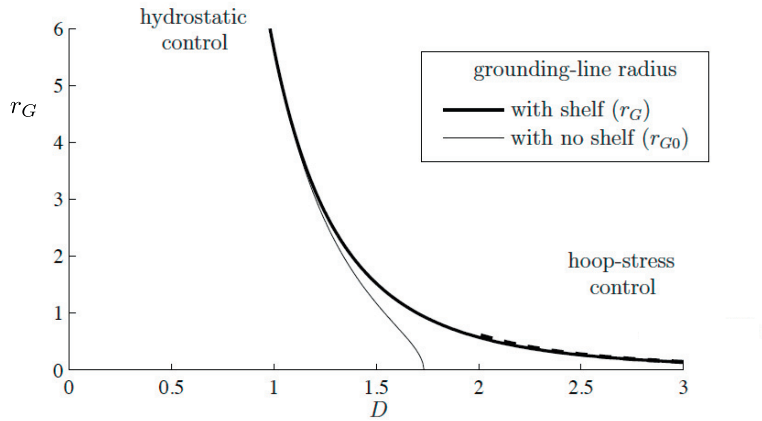

Fig. 8. Steady positions of a radial grounding line in oceans of different depths. When a shelf is present then steady grounding lines are achieved for all depths of ocean. There is no steady state if the shelf is absent in a deep ocean.

The most significant insight revealed by analysis of this system is that the buttressing hoop stresses in the shelf allow steady grounding lines for all depths of ocean (Fig. 8) but that if the shelf is removed and the ocean is sufficiently deep ($D > \sqrt{3}$) then the grounding line recedes all the way to the origin – the ice sheet is no more!

Experiments have confirmed these predictions of the initial evolution of the grounding line and the front of the shelf (Fig. 9) but, despite every effort to control possible extenuating effects, show that the grounding line of an axisymmetric sheet fed by a constant flux continues to advance where the theory presented above predicts that it should have reached a steady position. Having carefully evaluated and eliminated from

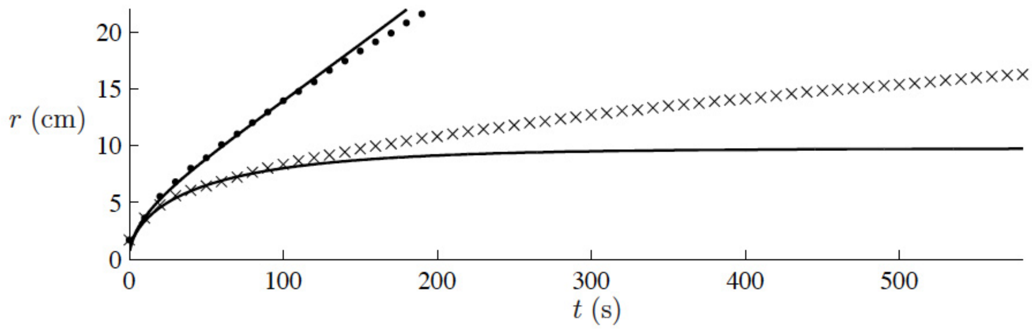

Fig. 9. Comparison between laboratory measurements and theoretical predictions for the positions of the grounding line (lower data and curve) and the front of the shelf (upper data and curve).

consideration a number of other potential causes for this observation, we are left with the conclusion that this discrepancy is a consequence of the neglect of viscous bending stresses in the neighbourhood of the grounding line.

5. Non-Newtonian, axisymmetric viscous gravity currents

Ice sheets are typically modelled as having a simple shear-thinning (power-law) rheology with a dynamic viscosity given by

$$\mu = \tilde{\mu}\left(\tfrac{1}{2}\boldsymbol{E} : \boldsymbol{E}\right)^{\left(\frac{1}{n}-1\right)/2}, \tag{26}$$

where $\boldsymbol{E}$ is the rate-of-strain tensor and $\tilde{\mu}$ is a material constant. This makes the equations employed in most studies algebraically cumbersome, though it is often the case that they are structurally similar to the more transparent equations describing Newtonian flow. There is little discussion of whether the shear-thinning rheology causes qualitatively different behaviour relative to that of a Newtonian fluid or is simply believed to give quantitative accuracy to the predictions of dynamically similar flows.

Consider, for example, the flow of an axisymmetric gravity current fed from a point source with constant flux Q_0. The leading-order dynamical equation, expressing a balance between vertical shear stresses and horizontal buoyancy gradients, is

$$\frac{\partial}{\partial y}\left(\mu\frac{\partial u}{\partial y}\right) \approx \rho g \frac{\partial h}{\partial r}, \tag{27}$$

which has solution

$$u = 2^{1-n}\left(\frac{\rho g'}{\tilde{\mu}}\right)^n \left(-\frac{\partial h}{\partial r}\right)^n \frac{h^{n+1}}{n+1}\left[1-\left(1-\frac{y}{h}\right)^{n+1}\right]. \tag{28}$$

This profile is topologically similar to the parabolic profile of a Newtonian current ($n = 1$), though the shear is a little more concentrated towards the base. Conservation of mass leads to the nonlinear diffusion equation

$$\frac{\partial h}{\partial t} + \frac{2^{1-n}}{n+2}\left(\frac{g}{\tilde{\nu}}\right)^n \frac{1}{r}\frac{\partial}{\partial r}\left[rh^{n+2}\left(-\frac{\partial h}{\partial r}\right)^n\right] = 0 \tag{29}$$

for the thickness $h(r,t)$ of the current. Given the constraint

$$2\pi\int_0^{r_N(t)} rh\,\mathrm{d}r = Q_0 t. \tag{30}$$

on the volume of the current, this equation admits a similarity solution in which

$$r_N \propto t^{(2n+2)/(5n+3)}. \tag{31}$$

For the complete range of shear-thinning fluids ($n \geqslant 1$), the exponent of time only varies between 0.5 ($n = 1$) and 0.4 ($n \to \infty$). For $n = 3$, the value favoured by ice modellers, the value of the exponent is 0.44. We see in this example that the shear-thinning model has made a slight quantitative difference to the predicted spreading rate but has introduced no new physical phenomenology. This is confirmed by experiments, which show perfectly axisymmetric spreading using golden syrup ($n = 1$) or a 1% by weight solution of Xanthan gum ($n \approx 5$).

6. Non-Newtonian sheet–shelf systems fed from a point source

In any theoretical model of viscous flows with defined geometry, be it two-dimensional or axisymmetric or confined to a channel for example, predictions made using power-law rheology are likely to be phenomenologically similar to those made using Newtonian rheology. But what if the geometry is unconstrained? We have conducted experiments in which viscous solutions of Xanthan gum were introduced from a point source into a layer of relatively dense, inviscid fluid – non-Newtonian versions of the system described in Sect. 4 above.

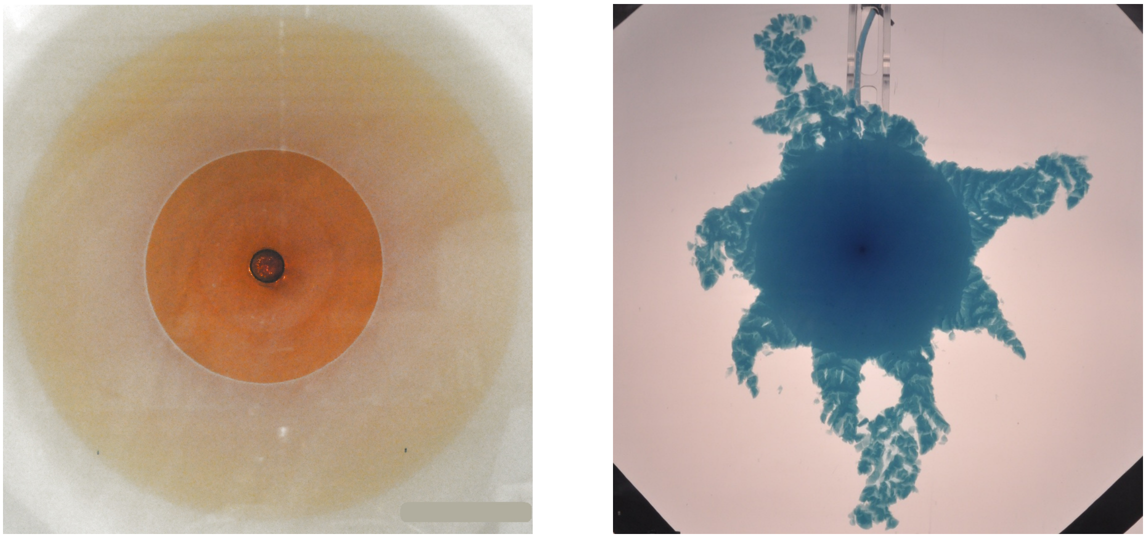

Fig. 10. Views from below of sheet-shelf systems spreading from point sources. With a Newtonian fluid (golden syrup, left image), the sheet (centre, bright orange) and shelf (annular, pale orange) remain axisymmetric. With a non-Newtonian fluid (Xanthan gum, right image), the sheet remains axisymmetric but the shelf fragments.

A theoretical model of this non-Newtonian system can be constructed and solved straightforwardly assuming that the flow remains axisymmetric. Such a model would reveal broadly similar physical balances and evolution to the Newtonian version of the problem, just as did the model of non-Newtonian gravity currents described in Sect. 5. However, the experiments reveal startlingly different behaviour, as shown in Fig. 10. Whereas the grounded sheet remains axisymmetric, the floating shelf fragments into quasi-radial fingers, which themselves break up into bergs. The axisymmetric flow is clearly unstable. It is currently an open problem whether the instabilities observed experimentally can be described using power-law rheology or whether a more complex, perhaps visco-elastic, rheology is required.

7. Conclusions

Scientific prediction relies on robust theoretical models tested against observation and experiment. In modelling the components of the Earth's climate system, we can sometimes use measurements of climate

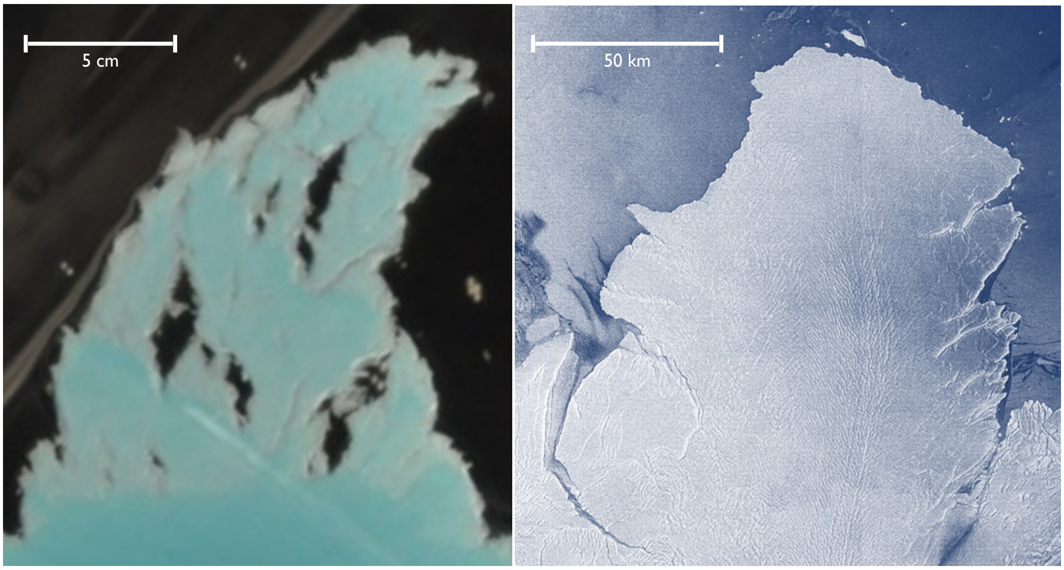

Fig. 11. Aerial views of a a tongue of Xanthan gum formed in a laboratory experiment and b the Stancomb–Wills ice tongue, Antarctica.

proxies to constrain the models we construct but cannot conduct our own planetary-scale experiments. Often, therefore, models are advanced based on sound physical principles but nevertheless making assumptions regarding what elements of a system are dominant in determining behaviour. The aim of the studies described here has been to develop theory of marine ice sheets step by step, testing each component rigorously in the laboratory and exploring the fundamental physical balances involved using asymptotic analysis. More sophisticated models than we have presented exist and in that sense we have taken a step back in order to be able to step forwards with much more confident footing.

Our analyses of Newtonian sheet–shelf systems have established principles that govern whether or not a shelf forms at the terminus of an ice sheet that flows into the ocean and have illustrated ways in which an ice shelf can buttress an ice sheet and stabilize its grounding line. However, the comparison between theory and experiment for an axisymmetric sheet–shelf system suggests that simple shallow-ice models may be inadequate to describe the dynamical evolution of grounding lines in all circumstances.

Finally, our experiments using shear-thinning fluids, which are exemplars of the rheology most commonly assumed by ice-sheet modellers, exhibit phenomenology that is visually similar to that observed in Antarctic ice shelves (Fig. 11). Whether these observations have a similar dynamical cause is the subject of ongoing research.

Acknowledgments

I am grateful to Sam Pegler and Roiy Sayag, not only for their significant research efforts that contributed to the studies described here but also for their careful reading of an earlier draft of this paper.

References

[1] Robison RAV, Huppert HE, Worster MG. Dynamics of viscous grounding lines, *J Fluid Mech* 2010; **648**: 363–380.
[2] Sayag R, Pegler SS, Worster MG. Floating extensional flows, *Phys Fluids* 2012; **24**: 091111.
[3] Pegler SS, Worster MG. Dynamics of a viscous layer flowing radially over an inviscid ocean, *J Fluid Mech* 2012; **696**: 152–174.
[4] Sayag R, Worster MG. Axisymmetric gravity currents of power-law fluids over a rigid horizontal surface, *J Fluid Mech* 2013; **716**: *R*5.
[5] Pegler SS, Worster MG. Dynamics of curved grounding lines, *J Fluid Mech* (In preparation).